JOURNAL OF CATALYSIS 144, 333–347 (1993)

Oxidative Coupling of CH_4 on Ag Catalyst-Electrodes Deposited on ZrO_2 (8 mol% Y_2O_3)

P. TSIAKARAS AND C. G. VAYENAS

Institute of Chemical Engineering & High Temperature Chemical Processes, Department of Chemical Engineering, University of Patras, Patras GR-26500, Greece

Received October 28, 1992; revised June 23, 1993

The oxidative coupling of CH_4 was investigated on polycrystalline Ag films deposited on yttria-stabilized zirconia (YSZ) at temperatures 720 to 850°C. It was found that electrochemical supply or removal of O^{2-} to or from the catalyst film results in very significant changes in both the rate of CH_4 consumption and in the product selectivity. For high CH_4-to-oxygen ratios, electrochemical supply of O^{2-} causes up to 50-fold increases in the rate of CH_4 consumption with a concomitant decrease in C_2 hydrocarbon selectivity. Electrochemical removal of O^{2-} causes a decrease in the rate of CH_4 consumption and an increase in C_2 selectivity. Electrochemically supplied oxygen can be significantly more active and selective than gas-phase oxygen. By varying the imposed current and catalyst potential the selectivity to C_2 hydrocarbons is varied reversibly between 25 and 75%. Maximum C_2 hydrocarbon yield was 8%. Due to the high operating temperatures, direct electrocatalysis and homogeneous reactions, more than NEMCA, affect the overall kinetic behaviour.

INTRODUCTION

Starting with the initial work of Keller and Bhasin (*1*), the reaction of oxidative coupling of methane (OCM) has been the focal point of several hundred studies which have examined more than a hundred catalytic materials (*2–5*). Since the pioneering work of Ito and Lunsford (*4*), it is generally believed that the main role of the catalyst surface is to generate $CH_3\cdot$ radicals which then combine primarily in the gas phase to generate C_2H_6. Due to its hetero-homogeneous nature, the OCM system is difficult to study in detail. Increasing CH_4 conversion always causes substantial losses in selectivity to C_2 hydrocarbons, due to the higher combustion reactivity of C_2H_4 and C_2H_6, thus maximum C_2 yield is of the order of 25%.

The electrochemical oxidation of CH_4 to C_2 hydrocarbons utilizing solid electrolyte YSZ cells offers in principle several advantages (*6*). First dioxygen is, in principle, not introduced in the gas phase, thus eliminating the homogeneous pathways leading to CO_x formation. Second, oxygen is introduced as O^{2-}, which is still believed by several workers to be the active oxygen species for hydrogen abstraction from CH_4 to generate $CH_3\cdot$ and thus initiate the OCM reaction. Thus, starting from 1985, Otsuka *et al.* (*7–10*) and Stoukides and co-workers (*11–13*) and others (*14, 15*) have explored the use of YSZ solid electrolyte cells with Ag, Bi_2O_3/Ag (*7*), $LiMgO_x$/Ag (*8*), Au (*12*), LiCl/NiO (*8*), and $LiNiO_2$ (*9*) anodes for the OCM process. Work in this area has been reviewed recently (*6*). With the exception of that for the LiCl/NiO electrode (*8*), all other studies showed a decrease in C_2 selectivity with increasing rate of O^{2-} supply, although electrochemically supplied oxygen was shown to be more active than gas-phase supplied oxygen (*7*).

It has been recently found that solid electrolytes, such as YSZ and β''-Al_2O_3, can act as active catalyst supports and alter dramatically the catalytic activity and selectivity of supported metal films upon polarizing the

0021-9517/93 $5.00

metal–solid electrolyte interface (*16–37*). This effect of non-Faradaic electrochemical modification of catalytic activity (NEMCA) (*16–37*) or "Electrochemical Promotion in Catalysis" (*39*) has been studied already at temperatures 200 to 650°C for over 20 catalytic reactions on Pt, Pd, Rh, Ag, and Ni utilizing O^{2-} (*17–24, 26–35*), Na^+ (*16, 25*), H^+ (*36*), and more recently F^- (*37*) conducting solid electrolytes. It has been shown that the rate of catalytic reactions can be reversibly enhanced by up to a factor of 60 (*16, 17*) and that the steady-state rate increase can be up to a factor of 3×10^5 higher than the rate of supply of O^{2-} (*16, 17*). In all NEMCA studies of catalytic oxidations, oxygen was, of course, admixed in the gas phase, which was not the case in most previous solid electrolyte OCM studies, with some exceptions (Refs. (*8, 9, 12, 13*)).

The present work is part of an investigation attempting to utilize solid electrolyte supports and NEMCA to promote methane conversion to C_2 hydrocarbons on metal and metal oxide catalysts (*29, 38, 40*). The work of Otsuka *et al.* on $LiNiO_2$ utilizing a two-electrode system has indeed shown (*9*) that when O_2 is admixed in the gas phase then the increase in its rate of consumption upon O^{2-} pumping can exhibit some non-Faradaic behaviour, i.e., enhancement factor Λ values (*16, 17*) up to 2.7 (*6*).

Unlike previous studies which used a two-electrode configuration, the present one utilizes a three-electrode system so that catalyst potential (17–34) and work function changes (*16, 17*) can be measured. Also, the effect of both positive and negative currents on the rate of CH_4 consumption and on C_2 selectivity and yield is studied in detail.

EXPERIMENTAL

The apparatus (Fig. 1). utilizing gas chromatography and IR-spectroscopy (Anarad analyzers for CH_4 and CO_2) for reactant and product analysis has been described in previous papers (*17–21*). The carbon balance closure was typically within 1% and there

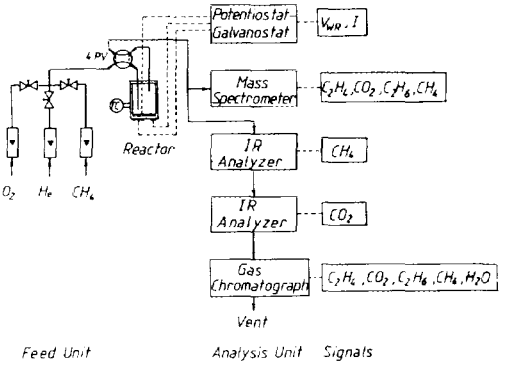

FIG. 1. Schematic of the apparatus.

was no sign of any significant coke deposition even at the highest temperatures and CH_4-to-O_2 ratios used. The YSZ (8 mol% Y_2O_3 in ZrO_2), atmospheric pressure, continuous flow well mixed (CSTR) reactor has a volume of 30 cm^3 and has also been described previously (*17–21*). Results reported here are typically obtained with total flowrates of 1–3 cm^3 STP/s. Reactants were Air Liquide certified standard CH_4 in N_2 and Air Liquide 20 mol% O_2 in N_2. They could be further diluted in pure N_2 (99.99%).

The Ag catalyst film was deposited on the inside bottom wall of the YSZ tube by applying a thin coating of Ag solution in butyl acetate (GC electronics) followed by drying and then calcining in air, initially at 200°C for 2 h, then at 400°C for 2 h, and finally at 880°C for 30 min. This high sintering temperature was necessary since the catalyst had to operate at temperatures up to 850°C. Furthermore, high sintering temperatures lead to larger Ag crystallites thus decreasing the three-phase-boundary length YSZ–Ag–air and thus decreasing the exchange current I_0 of the YSZ–Ag interface (*17*), which is known to be necessary in NEMCA studies (*17–34*).

Two Ag catalyst films, labeled C1 and C2, were used in the course of the experiments and both gave similar results in terms of Λ and r/r_0. Their active catalytic surface areas were measured by measuring their reactive oxygen uptake N_O via surface titration of

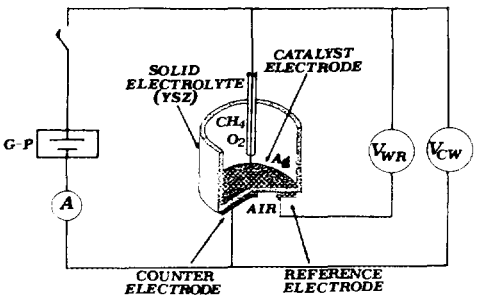

FIG. 2. Catalyst plus counter and reference electrode configuration.

O_2–CO at 400°C (*17, 18, 32, 33*). The value of N_O was found to be 5×10^{-7} and 3×10^{-8} gatom O, for the two films respectively. The films were also characterized by measuring the exchange current I_0 of the catalyst-solid electrolyte interface. The experimental procedure for extracting I_0 from current vs overpotential (Tafel) plots has been described in detail elsewhere (*17*). The results are presented below.

Two similar Ag films were deposited on the outside wall of the stabilized zirconia tube which was exposed to ambient air (Fig. 2) and served as counter and reference electrodes, respectively. In the course of the experiments both galvanostatic and potentiostatic operation was used, by means of an AMEL 553 galvanostat–potentiostat, and both gave similar results. In the galvanostatic mode a constant current I is applied between the catalyst and the counter-electrode while monitoring the ohmic-drop-free (*17–34*) catalyst potential V_{WR} between the catalyst and the reference electrode. To obtain V_{WR} one must subtract from the measured V'_{WR} value the parasitic working-reference $(IR)_{WR}$ ohmic drop (*17*). The procedure for doing this via the current interruption technique and utilizing a memory oscilloscope (Hameg HM-205) has been described previously (*17*). In the present work, and due to the high operating temperatures, $(IR)_{WR}$ was found to be typically less than 5 mV and was thus neglected in subsequent measurements. In the potentiostatic mode a constant potential V_{WR} is applied between the catalyst and the reference electrode while monitoring the current I between the catalyst and the counter electrode.

RESULTS

A set of blank experiments performed in absence of the Ag catalyst revealed that the YSZ solid electrolyte is a reasonably active and selective catalyst for the OCM reaction. These results together with kinetic measurements obtained with YSZ powder have been discussed elsewhere (*41*). The turnover frequency of CH_4 conversion on YSZ under the temperature and gas composition conditions employed here is typically 2×10^{-2} molecules CH_4/(surface Zr atom) · s (*41*). This corresponds to rate values of at most 10^{-9} mol/s in the present reactor arrangement. In view of the fact that measured CH_4 conversion rates in presence of the Ag catalyst were 10^{-8}–10^{-7} mol/s one can, to a good approximation, neglect the rate due to the solid electrolyte.

Figure 3 shows the effect of CH_4 partial pressure P_{CH_4} on the rates of formation of

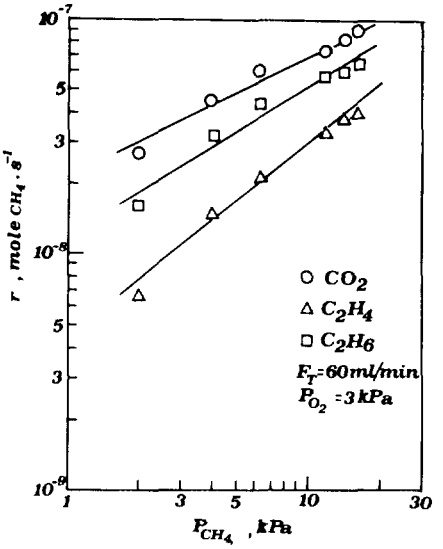

FIG. 3. Effect of P_{CH_4} on the rates of formation of C_2H_6, C_2H_4, and CO_2; P_{O_2} = 3 kPa, T = 835°C, catalyst C1, total oulet volumetric flowrate F_t = 60 cm³ STP/min.

C_2H_6, C_2H_4, and CO_2 at constant P_{O_2} over the Ag catalyst. The apparent reaction orders with respect to methane are 0.7, 0.8, and 0.55 for C_2H_6, C_2H_4, and CO_2 formation, respectively.

The effect of P_{O_2} at constant P_{CH_4} is shown in Fig. 4. The apparent reaction orders with respect to oxygen are 0.7, 1.3, and 0.9, respectively, for C_2H_6, C_2H_4, and CO_2 formation. The significantly higher reaction order for C_2H_4 vs C_2H_6 formation suggests that, indeed, C_2H_4 is a secondary reaction product resulting from the oxidative dehydrogenation of C_2H_6. This is also supported by the very high apparent activation energy for C_2H_4 formation (80 kcal/mol vs 48 and 40 for C_2H_4 and CO_2, respectively (*43*) which suggests a predominantly homogeneous pathway for the dehydrogenation reaction.

Current–potential behaviour. Figure 5 shows the effect of catalyst overpotential η on current I. The overpotential η is defined from

$$\eta = V_{WR} - V^{o}_{WR}, \qquad (1)$$

where V^{o}_{WR} is the open-circuit catalyst potential relative to the reference electrode. Positive overpotentials ($\eta > 0$) cause an exponential increase in current ($I > 0$) and thus in the rate $I/2F$ of O^{2-} supply *to* the catalyst. This exponential (Tafel) dependence is in good agreement with the high-field approximation of the Butler–Volmer equation (*17, 20, 21*), i.e., with

$$\ln (I/I_0) = \alpha_a F\eta/RT, \qquad (2)$$

where I_0 is the exchange current of the metal–solid electrolyte interface and α_a is the anodic transfer coefficient, with a value near 2 for the present system (Fig. 5).

Negative overpotentials ($\eta < 0$, $I < 0$) lead to limiting current behaviour, i.e., the current approaches a limiting, mass-transfer limited, value I_L (Fig. 5) and thus no Tafel (exponential) behaviour is observed. This behaviour is due to the low value of P_{O_2}.

The measured apparent activation energy of I_0, i.e., 21 kcal/mol (*43*) is in good agreement with literature values obtained for Ag obtained in presence of O_2 only (*17*).

The measured (*43*) apparent activation

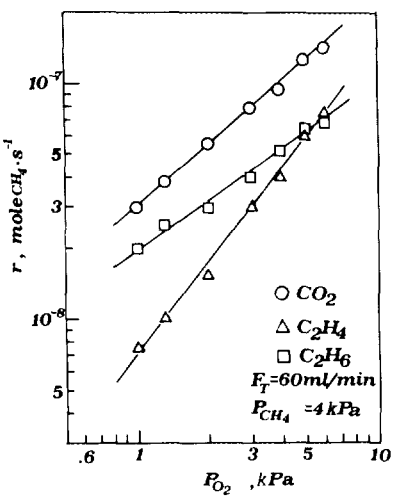

FIG. 4. Effect of P_{O_2} on the rates of formation of C_2H_6, C_2H_4, and CO_2; P_{CH_4} = 4 kPa, T = 835°C, catalyst C1, F_t = 60 cm³ STP/min.

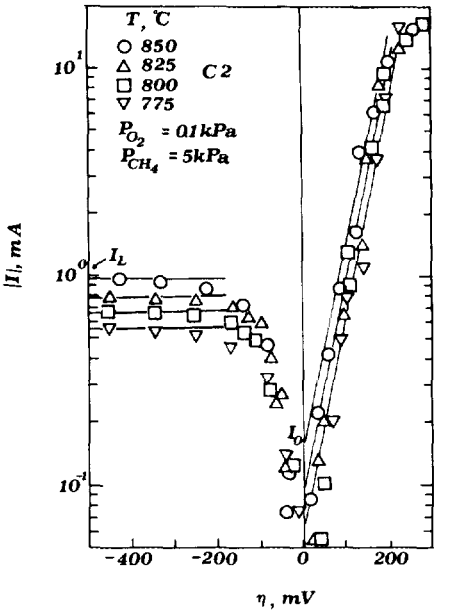

FIG. 5. Effect of catalyst overpotential η on current; Catalyst C2. Straight lines for $\eta > 0$ from Eq. (2).

energy for I_L was also high (17 kcal/mole) suggesting that the limiting current behaviour is not due to gas-phase diffusional limitations but rather to surface diffusion on the Ag catalyst film and bulk diffusion through the film, which has a substantial oxygen solubility at these elevated temperatures (*33*, *42*). It is likely that this oxygen solubility plays an important role in the OCM reaction, as discussed below.

Similarly to the case of the other known OCM catalysts, high operating temperatures (700–850°C) are necessary to activate CH_4 on Ag. These high temperatures cause the measured high values of I_0.

Previous NEMCA studies (*16–34*) have shown that one can estimate the order of magnitude of the absolute value $|\Lambda|$ of the enhancement factor Λ, defined by

$$\Lambda = \Delta r/(I/2F) \tag{3}$$

on the basis of the approximate expression

$$|\Lambda| = 2Fr_0/I_0, \tag{4}$$

where r_0 is the open-circuit catalytic rate. The derivation of Eq. (4) has been presented in detail elsewhere (*17*). The good agreement between Eq. (4) and experiment is shown in Fig. 6, which depicts measured Λ values for 15 catalytic reactions, including the present one. Due to the high operating temperatures and high I_0 values, the measured Λ values are small (Eq. (4)), typically less than 2, although for low applied currents Λ values up to 4 were also measured.

The physical origin of this can be understood as follows: when I_0 is high (say 0.2 mA), then currents I of 20 mA are required to cause a nontrivial catalyst overpotential of, say, 200 mV (Fig. 5 or Eq. (2)). However, the O^{2-} flux I/2F corresponding to 20 mA is 1.03×10^{-7} g-atom O/s, i.e., larger than the open-circuit catalytic rate which is typically 2×10^{-8} g-atom O/s. Thus even a tenfold rate increase will give Λ values of order 2. Therefore it is the combination of slow kinetics for CH_4 oxidation (low r_0) and high operating temperatures (high I_0) which

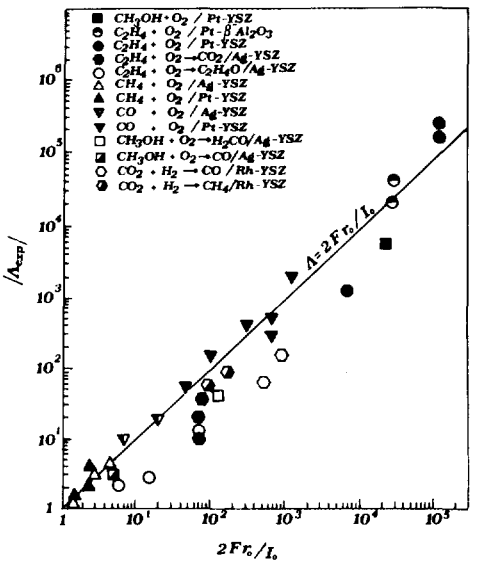

FIG. 6. Effect of the parameter $2Fr_0/I_0$ on the absolute value $|\Lambda|$ of the enhancement factor Λ for different catalytic reactions (see also Ref. (*17*)).

dictates the low magnitude of $|\Lambda|$. Consequently, as in the case of CH_4 oxidation on Pt (*38*), direct electrocatalysis is expected to strongly affect the overall kinetic behaviour during O^{2-} pumping.

Galvanostatic transients. Figures 7a, 7b, and 7c show typical galvanostatic transients, i.e., they depict the transient effect of step changes in applied current on the rate of CO_2 production r_{CO_2}. These rate transients were followed via the nondispersive IR CO_2 analyzer thus, unfortunately, the rates of ethane and ethylene production, $r_{C_2H_4}$ and $r_{C_2H_6}$, respectively, could not be continuously monitored. Product sampling and GC analysis showed, however, that they follow, qualitatively, the same transient behaviour.

Figures 7a and 7b depict the effect of positive currents at high (24 : 1) and very high (150 : 1) inlet CH_4-to-O_2 ratios. Such high ratios were found necessary to obtain high open-circuit selectivity to C_2 hydrocarbons and, consequently were chosen for investigating the effect of applied current and potential. Under these conditions and due to

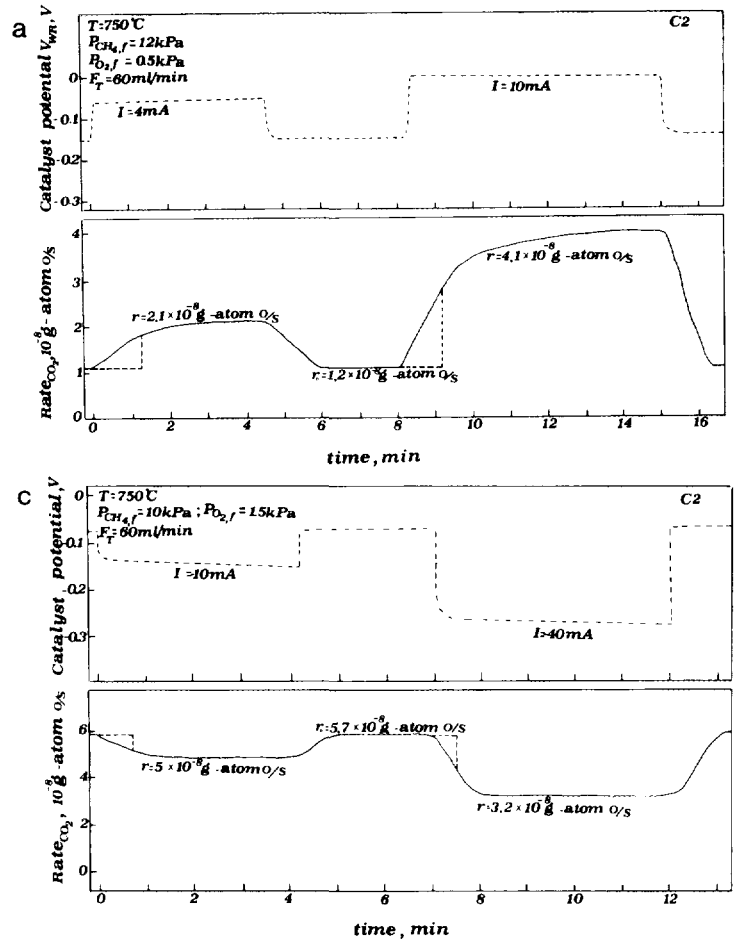

FIG. 7. Transient effect of step changes in applied current on the rate of CO_2 formation r_{CO_2}; catalyst C2. (a) Positive currents at high (24 : 1) CH_4-to-O_2 inlet ratio; maximum oxygen conversion is 10%. (b) Positive current at very high (150 : 1) CH_4-to-O_2 inlet ratio; maximum oxygen conversion is 88%. (c) Effect of negative currents; maximum oxygen conversion is 5%. See text for discussion.

the large effect of applied current described below, near complete conversion of totally supplied oxygen is often reached. Denoting by G the total inlet (feed) molar flowrate and by $y_{O_2,f}$ the inlet oxygen molar fraction, it follows that the total oxygen supply (g-atom/s) equals $(2G \cdot y_{O_2,f} + I/2F)$. Thus, because of the high inlet CH_4-to-O_2 ratios and high total oxygen conversions it was not practical to attempt to maintain P_{O_2} in the reactor constant upon varying the current or the catalyst potential. Consequently the experiments were performed under constant inlet CH_4 and O_2 values $P_{CH_4,f}$ and $P_{O_2,f}$. When desirable the corresponding P_{CH_4} and P_{O_2} values in the atmospheric pressure CSTR can be immediately computed at steady-state or during transients from the given values of total volumetric flowrate F_t (in cm^3 STP/min) together with the applied current and observed rate values. The two positive current transients shown on Figures 7a and 7b were chosen because the former corresponds to a Faradaic process ($\Lambda_{CO_2} < 1$) and the latter to a non-Faradaic one ($\Lambda_{CO_2} > 1$). The enhancement factors

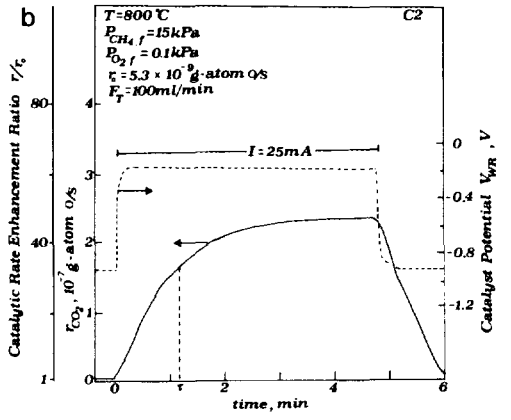

FIG. 7—*Continued*

$\Lambda_{C_2H_6}$, $\Lambda_{C_2H_4}$, Λ_{CO_2} are defined by

$$\Lambda_{C_2H_6} = \Delta r_{C_2H_6}/(I/2F) \quad (5a)$$

$$\Lambda_{C_2H_4} = \Delta r_{C_2H_4}/(I/2F) \quad (5b)$$

$$\Lambda_{CO_2} = \Delta r_{CO_2}/(I/2F), \quad (5c)$$

where, in order to keep the notation consistent with previous NEMCA studies, the rates $r_{C_2H_6}$, $r_{C_2H_4}$, and r_{CO_2} are expressed in g-atom O/s or g-equivalent O/s by using the stoichiometries of the three overall reactions:

$$2CH_4 + \tfrac{1}{2}O_2 \rightarrow C_2H_6 + H_2O \quad (6a)$$

$$2CH_4 + O_2 \rightarrow C_2H_4 + 2H_2O \quad (6b)$$

$$CH_4 + 2O_2 \rightarrow CO_2 + 2H_2O. \quad (6c)$$

It follows from the definitions of $\Lambda_{C_2H_6}$, $\Lambda_{C_2H_4}$, and Λ_{CO_2} that their sum equals Λ, i.e., the total enhancement factor for oxygen consumption.

As shown in Fig. 7a, the electrical circuit is initially open ($I = 0$) and the open-circuit rate of CO_2 formation r_{O,CO_2} is 1.2×10^{-8} g-atom O/s. The corresponding open-circuit catalyst potential value V^0_{WR} is -150 mV. At $t = 0$ the galvanostat is used to apply a constant current $I = 4$ mA, which corresponds to a rate of O^{2-} transfer to the catalyst of $I/2F = 2.1 \times 10^{-8}$ g-atom O/s. The catalyst potential V_{WR} changes rapidly to -60 mV, while r_{CO_2} gradually reaches a steady-state value of 2.1×10^{-8} g-atom O/s, which is 75% higher than r_{O,CO_2}, i.e., in this case it is $\rho_{CO_2} = r_{CO_2}/r_{O,CO_2} = 1.75$ and $\Lambda_{CO_2} = 0.45$. Upon current interruption r_{CO_2} returns to its open-circuit value, thus the effect is reversible.

Subsequent application of a larger positive current ($I = 10$ mA, $I/2F = 5.18 \times 10^{-8}$ g-atom O/s) causes a 240% increase in the rate ($\rho_{CO_2} = 3.4$) and a Λ_{CO_2} value of 0.56. The rate again returns to its open-circuit value upon current interruption (Fig. 7a).

Both the rate enhancement ratio ρ_{CO_2} and the enhancement factor Λ_{CO_2} increase substantially at higher CH_4 to O_2 ratios, as shown in Fig. 7b. Here the initial open-circuit ($I = 0$) value of r_{CO_2} is 5.3×10^{-9} g-atom O/s with $V^0_{WR} = -900$ mV. Application of a positive current ($I = 25$ mA, $I/2F = 1.3 \times 10^{-7}$ g-atom O/s) leads to $r_{CO_2} = 2.3 \times 10^{-7}$, i.e., r_{CO_2} increases by 4200%, thus $\rho_{CO_2} = 42$. The rate increase $\Delta r_{CO_2} = 2.25 \times 10^{-7}$ g-atom O/s is 73% higher than $I/2F$, i.e., $\Lambda_{CO_2} = 1.73$. Thus in the above case, even without taking into account that $r_{C_2H_6}$ and $r_{C_2H_4}$ are also increasing, the effect of current is non-Faradaic.

Figure 7c shows two examples of negative current application (O^{2-} removal from the catalyst). In the former case ($I = -10$ mA) it is $\rho_{CO_2} = 0.88$ and $\Lambda_{CO_2} = 0.14$. In the latter case ($I = -40$ mA) one obtains $\rho_{CO_2} = 0.56$ and $\Lambda_{CO_2} = 0.12$. As discussed below, negative currents lead to proportionally smaller decreases in $r_{C_2H_6}$ and $r_{C_2H_4}$, thus the C_2 selectivity increases.

Steady-state effect of current and potential. Positive currents, i.e., O^{2-} supply to the catalyst, was found to increase the rates of formation of C_2H_6, C_2H_4, and CO_2 with a concomitant decrease in selectivity to C_2 hydrocarbons from an open-circuit value $S_c \approx 0.55$–0.6 down to 0.25–0.30 and a concomitant increase in C_2 yield up to 8%. Typical results are shown in Fig. 8a, 8b (catalyst C1, different inlet CH_4 to O_2 ratios), and 8c (catalyst C2).

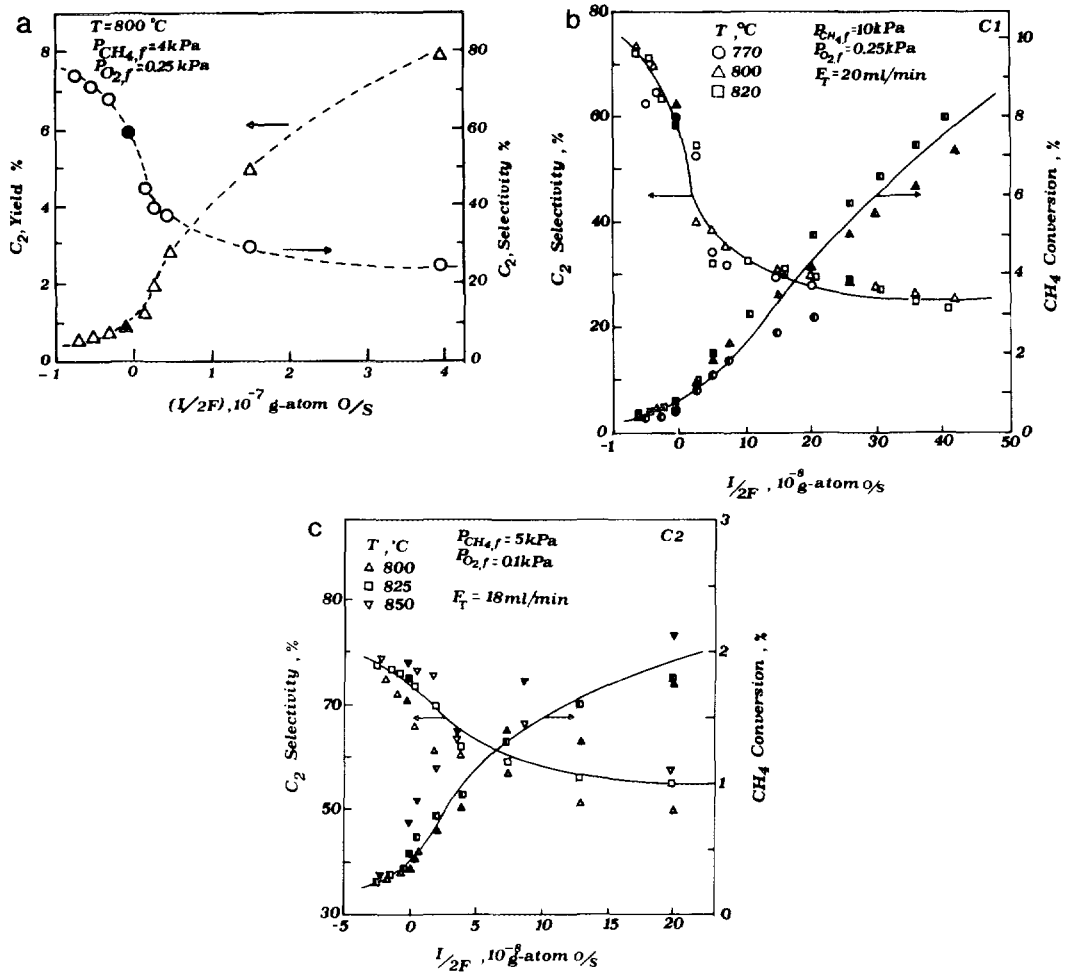

FIG. 8. (a) Effect of current on the selectivity and yield to C_2 hydrocarbons; F_t = 13 cm^3 STP/min; maximum oxygen conversion is 80%; catalyst C1. (b) Effect of current on CH_4 conversion (half-filled symbols) and C_2 selectivity (open symbols); catalyst C1. (c) Effect of current on CH_4 conversion (half-filled symbols) and C_2 selectivity (open symbols); catalyst C2.

As also shown in these figures negative currents cause an increase in C_2 selectivity up to 0.75–0.80 and a concomitant decrease in C_2 yield.

This behaviour can be rationalized on the basis of Figs. 9 and 10, which show typical results of the dependence of the rates of C_2H_4, C_2H_6, and CO_2 formation on catalyst potential V_{WR} and on applied current. Increasing V_{WR} and I causes an increase in the three rates in the sequence $\Delta r_{C_2H_6} < \Delta r_{C_2H_4} < \Delta r_{CO_2}$, thus in general causing a decrease in C_2 selectivity. As shown in Fig. 9, the rates of formation of C_2H_6, C_2H_4, and CO_2 vary exponentially with catalyst potential V_{WR}. This dependence can be expressed in terms of the dimensionless catalyst potential $\Pi = FV_{WR}/RT$ as

$$\ln (r_{C_2H_6}/r_{O,C_2H_6}) = \alpha_{C_2H_6}(\Pi - \Pi^*_{C_2H_6}) \quad (7a)$$

$$\ln (r_{C_2H_4}/r_{O,C_2H_4}) = \alpha_{C_2H_4}(\Pi - \Pi^*_{C_2H_4}) \quad (7b)$$

$$\ln (r_{CO_2}/r_{O,CO_2}) = \alpha_{CO_2}(\Pi - \Pi^*_{CO_2}), \quad (7c)$$

with $\Pi^*_{C_2H_6} \approx \Pi^*_{C_2H_4} \approx \Pi^*_{CO_2} = -3.5$ and

$$\alpha_{C_2H_6} = 0.4\ (\Pi > \Pi^*_{C_2H_6}); \quad \alpha_{C_2H_6} = 0.07\ (\Pi < \Pi^*_{C_2H_6}) \tag{8a}$$

$$\alpha_{C_2H_4} = 0.75\ (\Pi > \Pi^*_{C_2H_4}); \quad \alpha_{C_2H_4} = 0.15\ (\Pi < \Pi^*_{C_2H_4}) \tag{8b}$$

$$\alpha_{CO_2} = 1\ (\Pi > \Pi^*_{CO_2}); \quad \alpha_{CO_2} = 0.3\ (\Pi < \Pi^*_{CO_2}). \tag{8c}$$

The fact that the α coefficients (*17*) are smaller than the anodic transfer coefficient $\alpha_a(\approx 2)$ can explain why (*17*) the measured Λ values depicted in Fig. 10 are, in general, smaller than $2Fr_o/I_0$. An additional reason is that under these conditions, i.e., nearly complete oxygen conversion, the Λ values are also restricted by mass balance considerations, i.e., by the total supply of oxygen. As shown in Fig. 10, measured Λ values are typically on the order of 0.05, 0.1, and 1 for $\Lambda_{C_2H_6}$, $\Lambda_{C_2H_4}$, and Λ_{CO_2}, respectively.

In general, due to the heterohomogeneous nature of the OCM process and high oxygen conversions used in the present study no simple or unambiguous physicochemical meaning can be assigned to the measured α values, as in previous NEMCA studies (*17, 20, 23*), since in the present case they reflect not only surface properties of the Ag catalyst, but also the effect of oxygen addition in the gas phase. Thus, to a first approximation if all the OCM reaction were taking place homogeneously in the gas phase, then all three α values would be close to 2, i.e., would equal the anodic oxygen transfer coefficient. Thus the observed sequence ($\alpha_{C_2H_6} < \alpha_{C_2H_4} < \alpha_{CO_2}$) may simply reflect the increasing participation of gaseous oxygen in the formation of C_2H_4 and CO_2 while the main role of the surface is to generate $CH_3\cdot$ via reaction of methane with O^{2-} as analyzed in the Discussion.

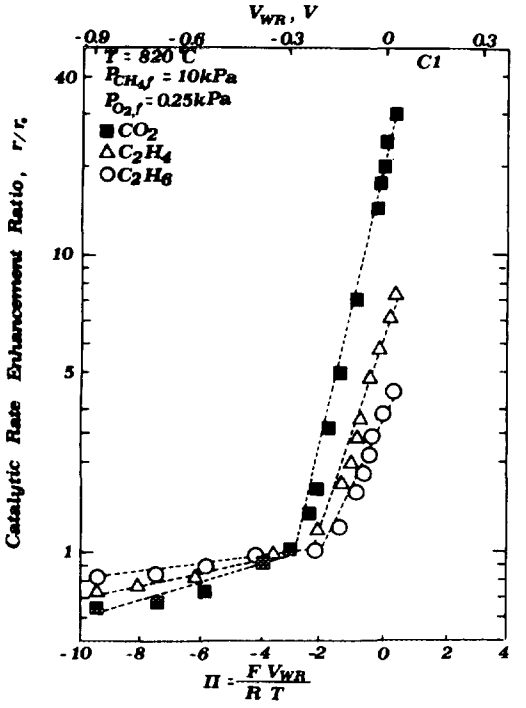

FIG. 9. Effect of catalyst potential on the rates of formation of C_2H_6, C_2H_4, and CO_2; catalyst C1, F_t = 30 cm^3 STP/min; maximum oxygen conversion is 90%.

Comparison of electrochemically supplied and gas-phase supplied oxygen. A question frequently addressed in the electrocatalytic OCM literature (*6–13*) is to what extent electrochemically supplied oxyagen (at a rate $I/2F$) is more active and selective than gas-phase supplied oxygen (at a rate $2G\cdot y_{O_2,f}$, *where* G is the total inlet molar flowrate and $y_{O_2,f}$ is the inlet oxygen mole fraction). As analyzed in discussion this question is usually not well-posed in the literature but, nevertheless, we felt it was worth addressing since the measured Λ values were small and since increasing V_{WR} and $I/2F$ is found to cause the same qualitative trends (increase in rates, decrease in C_2 selectivity) as increasing gas phase oxygen concentration does in nonelectrocatalytic OCM reactors.

Figure 11 is based on the data of Figs. 7a, 7b, 8a, and 10 referring to positive currents and shows the effect of total rate of oxygen supply ($2G\cdot y_{O_2,f} + I/2F$) on the total rate

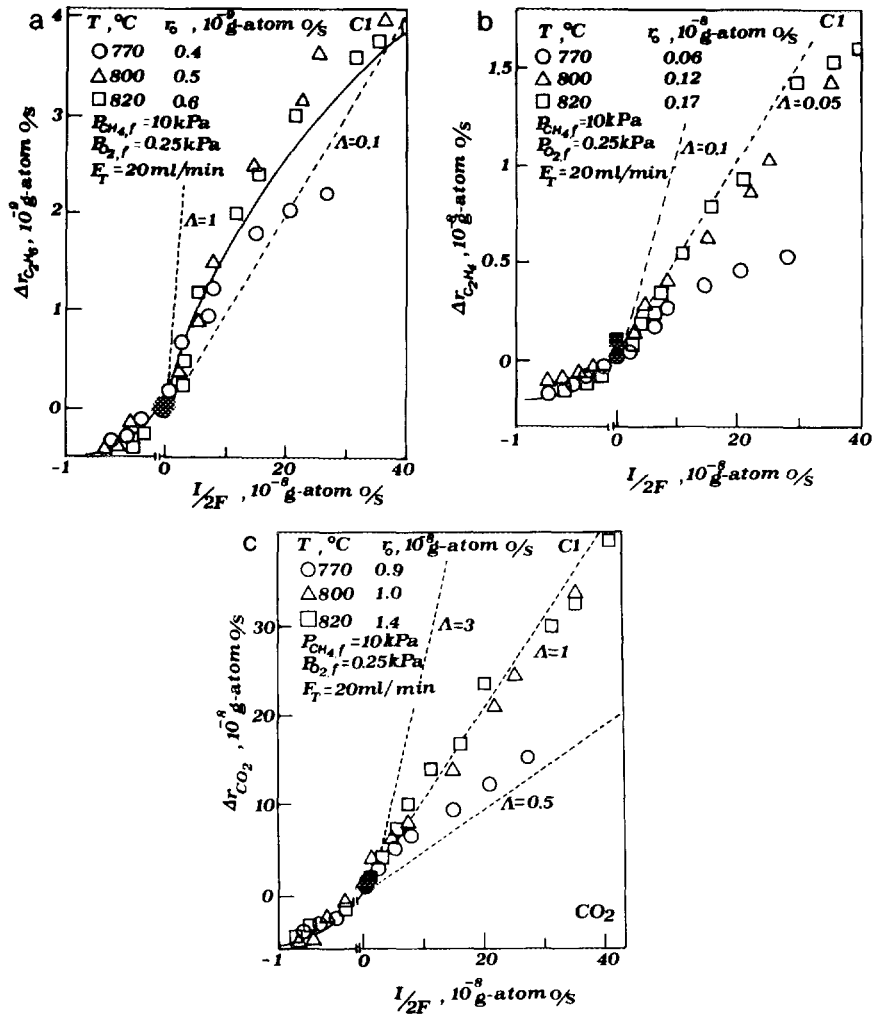

FIG. 10. Effect of current on the rate of formation of C_2H_6 (a), C_2H_4 (b), and CO_2 (c); dashed lines are constant enhancement factor Λ lines; catalyst C1.

of oxygen consumption. Open symbols in the figure correspond to pure gas-phase O_2 feed ($I = 0$), while filled symbols correspond to a mixed feed.

It is clear that mixed feed leads to total oxygen conversions which are typically 10 times larger than in the case of a pure-gas phase O_2 feed. Thus electrochemically supplied oxygen is to a first approximation 10 times more active than gas-phase supplied oxygen.

As shown in Fig. 12 electrochemically supplied O_2 is also more selective for C_2 formation than gas-phase oxygen. In this figure for each $y_{O_2,f}$ value a constant additional amount of oxygen has been electrochemically supplied ($I/2F$). Both modes of oxygen addition lead in general to a loss in C_2 selectivity but the loss is significantly more pronounced in the case of gas-phase supplied oxygen.

DISCUSSION

The present results show that Ag is a reasonably selective catalyst for the OCM reaction and that the rate of CH_4 conversion can be enhanced by up to a factor of 5000% by

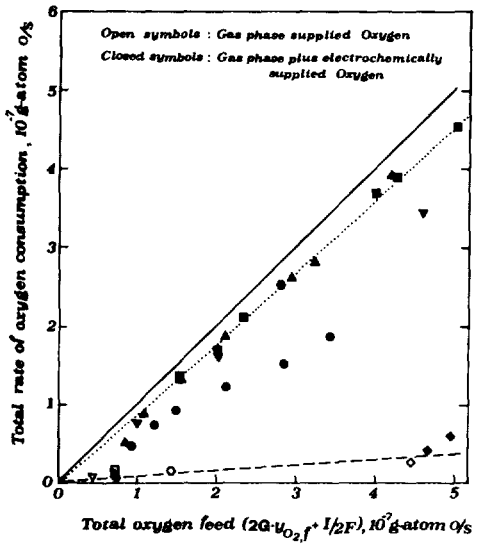

FIG. 11. Effect of total oxygen feed on the total rate of oxygen consumption; comparison between gas-phase oxygen supply (open symbols) and electrochemical plus gas-phase oxygen supply (filled symbols) (◇, from Figs 7a and 7b; ▽ from Fig. 8a; ○, △, □ from Fig. 10 (T = 770, 800, and 820°C, respectively)).

supplying O^{2-} via the YSZ solid electrolyte. The C_2 selectivity can be varied between 25 and 75%. Maximum C_2 yield was 8%, but this can very probably be improved by employing higher CH_4 conversions.

The ability of Ag to promote the OCM reaction at these elevated temperatures, where atomic oxygen adsorption on the Ag surface is practically nil (*33*, *34*), must be related to the finite solubility of oxygen in Ag (*33*, *42*). The solubility constant of oxygen on Ag and its diffusivity have been studied by material scientists using YSZ cells similar to the one used here (*42*). One computes from reference (*42*) that the solubility of oxygen in Ag at 800°C and at atmospheric pressure is 3.4×10^{-2} atom%. In a previous paper on the NEMCA effect during C_2H_4 epoxidation (*34*), we have discussed the possible relationship between this dissolved oxygen of material scientists and the subsurface oxygen of surface scientists (*44*), which is known to give broad TPD peaks at temperatures above 650°C (*44*, *45*).

This dissolved oxygen species hereafter denoted by O(d) is, the only oxygen species likely to survive near or on the Ag surface at these elevated temperatures and must be responsible for the abstraction of hydrogen from CH_4 and for the initiation of the OCM reaction:

$$CH_4 + O(d) \rightarrow CH_3\cdot + OH\cdot. \qquad (9)$$

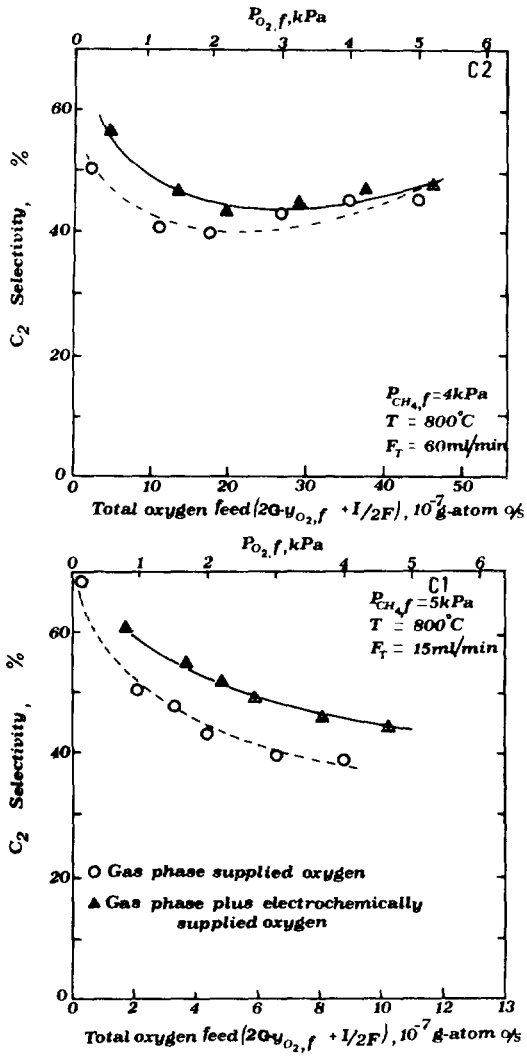

FIG. 12. Effect of total oxygen feed on C_2 selectivity; comparison between gas-phase oxygen supply (open symbols) and electrochemically plus gas-phase oxygen supply (filled symbols) at high (top) and low (bottom) flowrates and currents.

This is in agreement with the results of Anshits and co-workers (*46*, *6*) who used a silver membrane (0.13 mm thick) to supply oxygen for the OCM reaction and found that oxygen supplied through the Ag film was clearly more active and selective than gas-supplied O_2.

This is also supported by the present results (Figs. 11 and 12) which show that electrochemically supplied oxygen can be more active and selective than gas-supplied O_2. In a recent paper (*34*) we have discussed the main pathways followed by O^{2-} electrochemically supplied to Ag catalyst electrodes: a certain fraction of the O^{2-} flux forms covalently bonded chemisorbed atomic oxygen O(a) and eventually gaseous O_2:

$$O^{2-} \rightarrow O(a) + 2e^- \quad (10)$$

$$O(a) \rightarrow (1/2)\,O_2(g). \quad (11)$$

Another fraction, which increases with catalyst overpotential can form ionically bonded spillover ions O*, as evidenced by XPS (*47*, *48*), which spread over the catalyst surface and cause NEMCA:

$$O^{2-} \rightarrow O^* + 2e^- \quad (12)$$

$$O^* \rightarrow (1/2)\,O_2(g). \quad (13)$$

Reactions (10) and (12) take place at the three-phase boundaries (tpb) YSZ–Ag–gas (*34*). Reactions (11) and (13) are very fast at the high temperatures of the present study, leading to very low coverages of adsorbed and spillover oxygen, O(a) and O* respectively. In the case of Ag catalyst-electrodes, in addition to reactions (10) and (12) which occur at the tpb, there is a third charge transfer reaction taking place at the two-phase boundary YSZ–Ag and leading to formation of dissolved oxygen O(d):

$$O^{2-} \rightarrow O(d) + 2e^- \quad (14)$$

To the extent that the Ag crystallites are saturated with dissolved oxygen O(d), it follows that the occurrance of the charge transfer reaction (14) leads to the appearance of O(d) on the gas-exposed Ag surface giving rise to the OCM reaction according to reaction (9), i.e., the Ag film acts as a "sponge" for dissolved oxygen and supplies it at the Ag surface upon supplying O^{2-} at the YSZ–Ag interface.

Once $CH_3\cdot$ and $OH\cdot$ radicals have been generated and introduced to the gas phase via reaction (9), then they can react according to the general scheme established in classical catalytic OCM studies (*5*),

$$2\,CH_3\cdot + M \rightarrow C_2H_6 + M, \quad (15)$$

where M stands for a third body (*5*) which, conceivably, could be the surface itself (*2*).

$$CH_3\cdot + O_2 + M \rightarrow CH_3OO\cdot + M \quad (16)$$

$$CH_3OO\cdot + CH_4 \rightarrow CH_3OOH + CH_3\cdot. \quad (17)$$

According to this scheme CO_x products result from CH_3OOH combustion, while C_2H_4 results from C_2H_6 oxidative dehydrogenation.

Thus, according to the proposed reaction scheme for the system Ag–YSZ, dissolved oxygen O(d) formed at the YSZ–Ag interface is responsible for the initiation of the OCM reaction leading to C_2H_6 formation, while adsorbed and spillover oxygen forming at the tpb lead primarily to $O_2(g)$ evolution and to subsequent formation of C_2H_4 and CO_2.

It is worth noting that due to the heterohomogeneous nature of the OCM process, it is possible to obtain Λ values exceeding 1, even without changing the catalytic properties of the surface, as in NEMCA studies. Thus, considering the limit of zero overall C_2-selectivity, i.e., when CO_2 and H_2O are the only oxidation products, Λ can be as high as 4 if O^{2-} only generates $CH_3\cdot$ and $OH\cdot$ radicals (Eqs. (9) and (14) which are then converted to CO_2 and H_2O via gas-supplied oxygen. Thus even in the case of 50% C_2 selectivity, Λ values of the order of 2 can be obtained.

It appears therefore that the above simple kinetic scheme where Ag acts as a "sponge"

for dissolved oxygen which can generate $CH_3\cdot$ radicals on the Ag surface via reactions (9) and (14) can, to at least a first approximation, explain the observed kinetic behaviour.

The superior selectivity of electrochemically supplied vs gas-supplied O_2 is due to the fact that the former produces primarily O(d), while the latter, in addition to forming O(d), gets also involved in the homogeneous gas-phase reactions leading to formation of CO_2.

The observed decrease in selectivity with increasing current and potential is due to two factors: first, increased oxygen evolution in the gas phase and second the effect of increasing work function $e\Phi$ on the state of dissolved oxygen near the catalyst surface. Since dissolved oxygen is an electron acceptor, increasing $e\Phi$ weakens the Ag–O(d) bond near the Ag surface (*17*). This is known (*5*) to cause a decrease in selectivity, as strongly bonded oxygen is known to promote C_2 formation, while weakly bound oxygen is known to favor complete oxidation.

It is finally worth emphasizing some points where caution is needed when comparing the activity and selectivity of electrochemically and gas-phase supplied oxygen. The results presented in Fig. 11 show that electrochemically supplied oxygen is typically 10 times more active than gas-phase supplied oxygen. Previous workers have usually found smaller differences albeit in the same direction (Ref. (*6*) and references therein). When making such comparisons, attention must be paid to the following two points which are a very likely source of confusion in the literature.:

I. A true comparison can be made only when Λ is of order 1 or higher, as in the present case. This practically means for the present system using fuel-rich gas mixtures. For otherwise a fraction $(1-\Lambda)$ of the O^{2-} flux ends up in the gas phase (O_2 evolution). When Λ is less than, say, 0.1, then obviously no difference should be detected between gas-phase supplied and electrochemically supplied O_2, unless there are "reaction engineering" reasons for such a difference (non-ideal mixing, different residence time distributions, diffusional limitations).

II. The comparison between the rate caused by electrochemically supplied and gas-phase supplied oxygen, as usually done in the literature (*6*), is trully meaningful only when the catalyst surface area A is specified, which was not the case in previous studies. The rate, or rate increase, r_{el} due to electrochemically supplied oxygen is

$$r_{el} = \Lambda(I/2F), \tag{18}$$

while the rate r_{ch} due to gas-phase supplied oxygen is, in general,

$$r_{ch} = A \cdot k \cdot P_{O_2}^{\alpha} P_{CH_4}^{\beta}, \tag{19}$$

where k is a rate constant per unit surface A. Consequently the ratio ρ' of r_{el} and r_{ch} is

$$\rho' = \frac{\Lambda(I/2F)}{A \cdot k \cdot P_{O_2}^{\alpha} P_{CH_4}^{\beta}} \tag{20}$$

and can be made almost arbitrary large or small by appropriate choice of A. In the data shown in Fig. 11 it is typically $\rho' \approx 10$ with A of the order of 100 cm^2. However ρ' would decrease by 10 if A where to increase by 10. Similarly the ρ' values measured by previous workers would be a factor of 10 higher if the active gas-exposed catalyst-electrode surface were 10 times smaller. Thus ρ' values are only of engineering and not of any catalytic usefulness.

Consequently the only catalytically meaningful comparison of the activity of electrochemically and gas-phase supplied oxygen appears to be the comparison of their reaction probabilities. The reaction probability of electrochemically supplied O^{2-} is Λ, i.e., of the order of unity in the present study. The reaction probability of gaseous O_2 can be estimated from the kinetic theory of gases by dividing the observed rate of molecular O_2 consumption with the rate of O_2 impingement on the catalyst surface $P_{O_2}/(2\pi k_b m T)^{1/2}$. The reaction probability of O_2 is thus found to be of the order 5

$\times 10^{-9}$ in the present case. Thus each O^{2-} ion supplied electrochemically by the YSZ and then appearing on the Ag catalyst surface has 2×10^8 times higher probability to react with CH_4 than an O_2 molecule impinging on the same surface.

One aspect of the present work worth further investigation is the possible catalytic role of the YSZ electrolyte during O^{2-} pumping. Under open-circuit conditions the OCM rate on the YSZ accounted for less than 5% of the observed rate. However, to the extent that the Ag catalyst only acts as an oxygen "sponge" it is possible that the catalytic activity of the YSZ surface itself changes during O^{2-} pumping, at least in the vicinity of the Ag–YSZ interface, due to enhanced activity of O^{2-} for reaction with CH_4 to generate $CH_3 \cdot$ radicals.

SUMMARY

The catalytic activity of Ag films interfaced with YSZ for CH_4 oxidative coupling can be varied significantly by polarizing the Ag/YSZ interface and supplying or removing O^{2-} to or from the Ag catalyst. Due to the slow kinetics of CH_4 activation and the concomitantly high operating temperature and exchange current I_0, the role of NEMCA is limited and direct electrocatalysts, in addition to homogeneous gas-phase reactions, dominate the observed kinetic behaviour.

ACKNOWLEDGMENTS

Financial support by the EEC Non-Nuclear Energy and Joule Programmes is gratefully acknowledged. We also thank our reviewers for some valuable comments.

REFERENCES

1. Keller, G. E., and Bhasin, M. M., *J. Catal.* **73,** 9 (1982).
2. Hinsen, W., and Baerns, M., *Chem. Z.*, **107,** 223 (1983).
3. Driscoll, D. J., and Lunsford, J. H., *J. Phys. Chem.* **87,** 301 (1983).
4. Ito, T., and Lunsford, J. H., *Nature (London)* **314,** 721 (1985).
5. Lee, J. S., and Oyama, S. T., *Catal. Rev.-Sci. Eng.* **30**(2), 249 (1988).
6. Eng, D., and Stoukides, M., *Catal. Rev.-Sci. Eng.* **33,** 375 (1991).
7. Otsuka, K., Yokoyama, S., and Morikawa, A., *Chem. Lett. Jpn.*, 319 (1985).
8. Otsuka, K., Suga, K., and Yamanaka, I., *Catal. Lett.* **1,** 423 (1988).
9. Otsuka, K., Suga, K., and Yamanaka, I., *Chem. Lett. Jpn.*, 317 (1988).
10. Otsuka, K., Suga, K., and Yamanaka, I., *Catal. Today* **6,** 587 (1990).
11. Seimanides, S., and Stoukides, M., *J. Electrochem. Soc.* **133,** 1535 (1986).
12. Eng, D., and Stoukides, M., *Catal. Lett.* **9,** 47 (1991).
13. Eng, D., and Stoukides, M., *J. Catal.* **30,** 306 (1991).
14. Belyaev, V. D., Bazhau, O. V., Sobyanin, V. A., and Parmon, V. N., *in* "New Developments in Selective Oxidation" (C. G. Centi and F. Trifiro, Eds.), p. 469. Elsevier, Amsterdam, 1990.
15. Nagamoto, H., Hayashi, K., and Inoue, H., *J. Catal.* **126,** 671 (1990).
16. Vayenas, C. G., Bebelis, S., and Ladas, S., *Nature (London)* **343** (6259), 625 (1990).
17. Vayenas, C. G., Bebelis, S., Yentekakis, I. V., Lintz, H.-G., "Non-Faradaic Electrochemical Modification of Catalytic Activity: A Status Report", *Catal. Today* **11**(3), 303 (1992).
18. Yentekakis, I. V., and Vayenas, C. G., *J. Catal.* **11,** 170 (1988).
19. Vayenas, C. G., Bebelis, S., and Neophytides, S., *J. Phys. Chem.* **92,** 5083 (1988).
20. Bebelis, S., and Vayenas, C. G., *J. Catal.* **118,** 125 (1989).
21. Neophytides, S., and Vayenas, C. G., *J. Catal.* **118,** 147 (1989).
22. Vayenas, C. G., Bebelis, S., Neophytides, S., and Yentekakis, I. V., *Appl. Phys. A* **49,** 95 (1989).
23. Vayenas, C. G., Bebelis, S., Yentekakis, I. V., Tsiakaras, P., and Karasali, H., *Platinum Met. Rev.* **34**(3), 122 (1990).
24. Vayenas, C. G., and Neophytides, S., *J. Catal.* **127,** 645 (1991).
25. Vayenas, C. G., Bebelis, S., and Despotopoulou, M., *J. Catal.* **128,** 415 (1991).
26. Ladas, S., Bebelis, S., and Vayenas, C. G., *Surf. Sci* **251/252,** 1062 (1991).
27. Lintz, H-G., and Vayenas, C. G., Angew. Chem. **101,** 725 (1989); *Angew. Chem. Int. Ed. Engl.* **28,** 708 (1989).
28. Vayenas, C. G., Bebelis, S., and Neophytides, S., *in* "New Developments in Selective Oxidation" (G. Centi and P. Trifiro, Eds.), Studies in Surface Science and Catalysis, Vol. 55, p. 643. Elsevier, Amsterdam, 1990.
29. Vayenas, C. G., Bebelis, S., Yentekakis, I. V., Tsiakaras, P., Karasali, H., and Karavasilis, Ch., *ISSI Lett.* **2,** 5 (1991)

30. Vayenas, C. G., Bebelis, S., and Kyriazis, C., *Chemtech* **21,** 500 (1991)
31. Cavalca, C. A., Larsen, G., Vayenas, C. G., and Haller, G. L., *J. Phys. Chem.*, **97,** 6115 (1993)
32. Vayenas, C. G., Bebelis, S., Yentekakis, I. V., Tsiakaras, P., Karasali, H., and Karavasilis, Ch., *in* "Proc. 3d Intnl. Symp. on Systems with Fast Ionic Transport, Holzhau, Germany, 1991, "*Mater. Sci. Forum* **76,** 141 (1991); Tsiakaras, P., and Vayenas, C. G., 179; Karasali, H., and Vayenas, C. G., 171; Karavasilis, Ch., Bebelis, S., and Vayenas, C. G., 175; Bebelis, S., and Vayenas, C. G., 221.
33. Bebelis, S., and Vayenas, C. G., *J. Catal.* **138,** 570 (1992).
34. Bebelis, S., and Vayenas, C. G., *J. Catal.* **138,** 588 (1992).
35. Yentekakis, I. V., and Bebelis, S., *J. Catal.* **137,** 278 (1992).
36. T. I. Politova, V. A., Sobyanin, and V. D. Belyaev, *React. Kinet. Catal. Lett.* **41,** 321 (1990).
37. Yentekakis, I. V., and Vayenas, C. G., *J. Catal.*, submitted (1993).
38. Tsiakaras, P., and Vayenas, C. G., *J. Catal.* **140,** 53 (1993).
39. Pritchard, J., *Nature* **343,** 592 (1990).
40. Tsiakaras, P., and Vayenas, C. G., in preparation
41. Seimanides, S., Tsiakaras, P., Verykios, X. E., and Vayenas, C. G., *Appl. Catal.* **68,**41 (1991).
42. Ramanarayanan, T. A., and Rapp, R., *Metal Trans.* **3,** 3239 (1972).
43. Tsiakaras, P., Ph.D. thesis, University of Patras, 1993.
44. Van Santen, R. A., and Kuipers, H. P. C. E., *Adv. Catal.* **35,** 265 (1987).
45. Grant, R. B., and Lambert, R. M., *Surf. Sci.* **146,** 256 (1984)
46. Anshits, A. G., Shigapov, A. N., Vereshchagin, S. N., and Shevnin, V. N., *Catal. Today* **6,** 593 (1990).
47. Arakawa, T., Saito, A., and Shiokawa, J., *Chem. Phys. Lett.* **94,** 250 (1983).
48. Ladas, S., Kennou, S., Bebelis, S., and Vayenas, C. G., *J. Phys. Chem.*, in press (1993).